JOURNAL OF GEOPHYSICAL RESEARCH, VOL. 104, NO. D17, PAGES 21,537–21,547, SEPTEMBER 20, 1999

Effects of nonmethane hydrocarbons on lower stratospheric and upper tropospheric chemical climatology in a two-dimensional zonal average model

V. R. Kotamarthi[1]
Environmental Research Division, Argonne National Laboratory, Argonne, Illinois

D. J. Wuebbles
Department of Atmospheric Sciences, University of Illinois at Urbana-Champaign

R. A. Reck[2]
Environmental Research Division, Argonne National Laboratory, Argonne, Illinois

Abstract. The effect on the modeled chemical climatology of the upper troposphere and lower stratosphere of including a limited set of nonmethane hydrocarbons in a two-dimensional (2-D) zonal average model is presented. Recent measurements of nitrogenated and oxygenated hydrocarbons in the upper troposphere and lower stratosphere have revealed the possibility of significant perturbation of this region. A zonally averaged 2-D chemical transport model enhanced to represent tropospheric processes was used to explore the extent of this perturbation on global and regional spatial scales and on seasonal and annual average timescales. Acetone was shown to cause a significant increase in the HO_x budgets of the upper troposphere in the midlatitude Northern Hemisphere during the winter and early spring months, with acetone photolysis providing the most significant source of HO_x radicals. The tropical upper troposphere has a uniform increase in HO_x of up to 20% throughout the year because of acetone photolysis. Including the hydrocarbons caused a net increase in ozone of 5 ppbv in the lower and middle troposphere and 5–10 ppbv in the upper troposphere for global and annual averages. The effect of including the hydrocarbons on the calculated model ozone response for the case of doubled surface mixing ratios of atmospheric CH_4 is also discussed. It is shown that including hydrocarbons in the model has a significant effect on the modeled ozone response to the methane increase.

1. Introduction

The significance of nonmethane hydrocarbon (NMHC) chemistry in urban pollution events such as smog formation has been long recognized and intensively studied [*Seinfeld*, 1986]. The role of NMHC in the global-scale chemistry of the troposphere and lower stratosphere has attracted greater interest in recent years [*Kasting and Singh*, 1986; *Moxim*, 1996; *Singh et al.*, 1995; *McKeen et al.*, 1997; *Jaegle et al.*, 1997]. The effects of (1) long-lived hydrocarbons such as acetone on HO_x (H, HO_2, and HO) budgets, (2) peroxyacetyl nitrate (PAN) and similar odd nitrogen oxide reservoirs on NO_x (NO, NO_2) budgets, and (3) relatively short-lived hydrocarbons such as methylhydrogen peroxide (CH_3OOH) that are transported quickly into the upper troposphere by convective activity on HO_x production rates are under much debate [*Prather and Jacob*, 1997]. Even though the impacts of these hydrocarbons on the NO_x and HO_x cycles have been shown on the basis of point and air parcel chemistry models to be substantial, there is very little information on their global and annually averaged impacts. Several global-scale three-dimensional (3-D) chemical transport models (CTMs) with widely varying spatial resolution and representations of chemical mechanisms are quickly becoming available [*Brasseur et al.*, 1998; *Muller and Brasseur*, 1995; *Houweling et al.*, 1998; *Wang et al.*, 1998]. The 3-D CTMs designed for studying tropospheric chemistry include an extensive representation of hydrocarbon chemistry. However, detailed simulations to evaluate multiple scenarios are still a rarity with these models because of the extensive computer resources and costs involved. A few 2-D zonal average modeling studies of tropospheric chemistry have calculated hydrocarbon mixing ratios and their impacts on ozone and NO_x budgets [*Kanakidou et al.*, 1991; *Singh et al.*, 1994; *Strand and Hov*, 1994]. These modeling studies were successful in showing the importance of PAN as a NO_x reservoir in the winter months and the consequent impacts on ozone mixing ratios.

Here we will explore the role of acetone, ethane (C_2H_6), propane (C_3H_8), and related hydrocarbon compounds in the context of the 2-D zonal average model, used extensively in several assessment studies. The model, designed for stratospheric applications, was recently improved to give higher resolution in both the horizontal and vertical domains and has

[1]Also at the Department of Atmospheric Science, University of Illinois at Urbana-Champaign.
[2]Now at National Institute for Global Environmental Change, University of California, Davis.

Copyright 1999 by the American Geophysical Union.

Paper number 1999JD900334.
0148-0227/99/1999JD900334$09.00

sufficient resolution to represent the troposphere. Also addressed will be the effects of including NMHCs on perturbations in atmospheric chemistry resulting from an increase in methane [*World Meteorological Organization* (*WMO*) 1991, 1995] in a 2-D zonal average model climatology. The present study is relevant to the use of several model evaluations currently sponsored by National Aeronautical and Space Administration (NASA), WMO, Intergovernmental Panel on Climate Change (IPCC), and other organizations on the effects of such future perturbations on atmospheric chemistry and climate.

Several assessment studies have employed 2-D models to evaluate the effects of the expected increase in CH_4 (methane) concentrations on tropospheric oxidant levels [*WMO*, 1995]. Because of the long lifetime of CH_4 and the time it takes the CTM to achieve a steady state for the perturbed CH_4 calculations, it can be expected that the 2-D zonal average model will be used in the near future for this and similar applications. Therefore an evaluation of the impacts of introducing NMHCs and mixing processes relevant to the troposphere, at time and spatial scales of significance for 2-D models, will be of great value for future use of such models in these and similar applications. The present contribution needs to be evaluated in this spirit, not as an effort to simulate tropospheric processes in 2-D models in order to understand tropospheric chemical processes in detail.

1.1. Nonmethane Hydrocarbons in the Atmosphere

Hundreds of NMHCs have been measured in the atmosphere [*Blake et al.*, 1996; *Atlas et al.*, 1992; *Penkett et al.*, 1993]. Sources of hydrocarbons related to human activities include automobile exhaust, solvent usage, and biomass burning. Natural sources, especially trees, grasses, and shrubs, also generate a large number of hydrocarbons [*Guenther et al.*, 1995; *Fukui and Doskey*, 1998]. However, a vast majority of these compounds have been found to be rather short-lived with lifetimes between minutes and days as they tend to be highly reactive with HO in the atmosphere. Of the several hundred NMHCs emitted into the atmosphere, alkanes such as C_2H_6 and C_3H_8, alkynes such as C_2H_2 (acetylene), and some oxygenated compounds such as formaldehyde and acetone have lifetimes in excess of days and are available for transport on regional and global scales.

The fate of products of hydrocarbon decomposition is dominated by washout from the atmosphere with formation of highly soluble alcohols and peroxy radicals. One exception is PAN, a product of hydrocarbon decomposition that is recognized as a possible source of NO_x in the remote troposphere [*Moxim*, 1996, *Singh and Hanst*, 1981]. Recently, acetone has been added to the rather short list of hydrocarbon decomposition products with possible influence on the chemistry of the remote upper troposphere. Acetone has a significant direct source from human activities and thus could be considered in a somewhat different class than PAN.

There has been speculation about possible NO_x reservoir compounds formed from longer-chained organics and having longer lifetimes than the precursor hydrocarbons (so-called secondary pollutants). Measurements during certain periods in the arctic environment have shown that these NO_x-containing compounds can form close to 20% of the NO_y (sum of all odd nitrogen species in the gas phase) in the cold arctic environment [*Muthuramu et al.*, 1994]. Measurements in other parts of the world have not revealed a significant presence of these longer-chained organic nitrogen compounds [*Ridley et al.*, 1997].

1.2. NMHCs and Their Impact on Tropospheric Chemistry

The chemistry of NMHCs has been discussed in detail [*Seinfeld*, 1986; *Kasting and Singh*, 1986]. The pathways of interest to this study are as follows:

$$RH + OH \rightarrow RO_2 \quad (1)$$

$$RO_2 + NO \rightarrow NO_2 + RCHO + HO_2 + R\text{-}O\text{-}R \quad (2)$$

$$RCHO + OH \rightarrow RCO_3 \quad (3)$$

$$RCO_3 + NO_2 \rightarrow RCO_3NO_2 \quad (4)$$

$$RO_2 + NO_2 \rightarrow RO_2NO_2 \quad (5)$$

$$RO_2 + HO_2 \rightarrow ROOH \quad (6)$$

$$R\text{-}O\text{-}R + h\nu \rightarrow CH_2O + HO_2 \quad (7)$$

$$R\text{-}O\text{-}R + OH \rightarrow RCO_3 \quad (8)$$

$$ROOH + h\nu \rightarrow RO_2 + HO_2 \quad (9)$$

Previous studies [*Liu et al.*, 1987; *Kasting and Singh*, 1986] have explored in detail the reactions involved in increasing ozone levels. The oxidation of hydrocarbons gives rise to the peroxy radical, RO_2 (R1), where R is the carbon-containing fraction of the hydrocarbon formed on reaction with HO. This peroxy radical converts NO to NO_2, thus increasing the potential for ozone production. This is the major pathway for increases in ozone mixing ratios due to NMHCs in the lower troposphere, where hydrocarbons are abundant. Recognition that (7) could be an important source of HO_x radicals in the drier upper troposphere is recent, as discussed before. With the timescales of deep convective transport being revised to <10 days, products of reactions such as (9), transported to the upper troposphere under fast convective conditions, could become additional sources of HO_x [*Prather and Jacob*, 1997]. Reaction (4) leads to the formation of PAN and similar compounds that are thermally unstable at higher temperatures but are very stable, with lifetimes of the order of several months, in colder climates. Formation of NO_x reservoirs through (5), though feasible under atmospheric conditions [*Roberts*, 1990], has yielded mixed results in atmosphere measurements, as discussed in section 1.1. The significance of NMHC chemistry, even for remote tropospheric conditions, is thus becoming clear.

1.3. NMHCs in 2-D Zonal Average Models

Previous modeling studies of NMHCs include those of *Kanakidou et al.* [1991], *Strand and Hov* [1994], and *Singh et al.* [1995]. *Kanakidou et al.* [1991] explored the chemistry of ethane and propane with a 2-D zonal average tropospheric chemistry model using a detailed chemical representation of the oxidation reaction scheme for these compounds in the atmosphere. These authors explored in detail the formation of PAN, acetone, and other degradation products of C_2H_6 and C_3H_8 oxidation and their effects on the NO_x budget. Fixed surface mixing ratio boundary conditions, based on observations, were employed for C_2H_6 and C_3H_8. Their 2-D zonal average model, which was designed for tropospheric applications, extends from the surface to 25 km. The upper boundary conditions for ozone, NO_y, and other relevant trace gases are

based on the results of a companion stratospheric 2-D zonal average model and satellite observations.

Strand and Hov [1994] included a large set of hydrocarbons in their 2-D zonally averaged model and adapted a parameterized representation of hydrocarbon chemistry. *Strand and Hov* [1994] used flux boundary conditions in their calculations and explored several issues, including ozone budgets and NO_x chemistry. They also investigated the impacts of several emission reduction scenarios for hydrocarbons and nitrogen oxides on tropospheric ozone budgets. Their model is also designed for tropospheric applications and extends from the surface to 25 km [*Hough*, 1991]. A description of boundary layer processes and nonlocal deep convective mixing is included in this model. *Singh et al.* [1995] focused on the sources and sinks of acetone and methanol.

2. Model Description

The model used here is an extended form of the 2-D model originally developed at the Lawrence Livermore National Laboratory (and now at the University of Illinois at Urbana-Champaign) as discussed by *Wuebbles et al.* [1991] and *Kinnison et al.* [1994]. The model is zonally averaged, extending from pole to pole and from the surface to 85 km. The horizontal resolution is 5° latitude, and the vertical resolution is ~1.5 km. The model dynamics are calculated by using the residual mean circulation approach with National Center for Environmental Prediction (NCEP) temperature fields averaged over a 10-year period. The horizontal eddy mixing coefficients are calculated to be consistent with the circulation by using a planetary wave representation forced from the surface of the model [*Li et al.*, 1995]. Vertical mixing is set to give a turnover time of 1 month in the troposphere and is calculated on the basis of a gravity wave–breaking parameterization in the stratosphere and mesosphere. The model tropopause is fixed at an annual average value for the entire year. The base version of the model has full representation of ClO_x, BrO_x, NO_x, O_x, HO_x, CH_4, and CO chemistry relevant to stratospheric processes, and the reaction rates and photolytic cross-section are based on the recommendations of *DeMore et al.* [1997]. The chemistry module includes heterogeneous chemistry on sulfate aerosols and a parameterized representation of polar cloud chemistry. The photolytic rates are calculated with a two stream radiation model and updated every six days.

Surface level mixing ratios are specified for long-lived gases such as CH_4, N_2O, CFC-11, CFC-12, CH_3CCl_3, CH_3Br, and other halogen-containing gases. The surface level mixing ratios are set at 1.715 ppm for CH_4 at 300 ppb for N_2O, and at their current accepted levels in the troposphere, derived from the National Oceanic and Atmospheric Administration/Climate Monitoring and Diagnostics Laboratory (NOAA/CMDL) measurements, for other gases.

The current version of the model has an improved representation of the troposphere and includes a representation of the nonlocal convective mixing following the approach of *Strand and Hov* [1993] and *Prather et al.* [1987]. The convective mixing rates for deep and shallow convection on the 2-D zonal average model grid are based on the work of *Langner et al.* [1990]. We made several tests of the performance of the convective scheme by using radon 222 as a short-lived tracer and emission rates corresponding to the *Jacob et al.* [1997] evaluation of vertical tropospheric mixing rates in 2-D and 3-D models for the World Climate Research Program (WCRP).

Table 1. Surface Emission Fluxes of CO, NO_x, NMHCs Used in the Model

Compound	Emissions, Tg yr^{-1}
CO	1525
NO_x	40
C_2H_6	16.2
C_3H_8	26.8
Isoprene	450
Acetone	65
C_2H_2	10
C_3H_6	10

Our model results are similar to those of the 2-D zonal average model results from the Max Plank Institute, as expected (because the same convective mixing rates were used in that model). Besides CH_4, several other hydrocarbons, including C_2H_6, C_3H_8, C_2H_4, C_3H_6, isoprene, and their degradation products, are represented. Further details of the hydrocarbon chemistry are discussed below.

2.1. Hydrocarbon Chemistry

A selected set of NMHCs with lifetimes >1 day (for either the hydrocarbons or their degradation products) and with known impact on regional-scale chemistry [*Chang et al.*, 1987] were introduced into the model. Two alkanes (C_2H_6 and C_3H_8), two alkenes (C_2H_4 and C_3H_6), isoprene, and their degradation products were selected for the evaluation. The chemical scheme is a condensed version of the regional acid deposition model (RADM) chemical mechanism [*Chang et al.*, 1987] and follows *McKeen et al.* [1991]. Acetone photolysis rates employed were those of *Emrich and Warneck* [1988]. Reaction rates from *McKeen et al.* [1991] were updated on the basis of recommendations of the International Union of Pure and Applied Chemistry [*Atkinson et al.*, 1997]. A complete list of the reactions, reaction rates, and corresponding references is available at the following Web site: gandalf.atmos.uiuc.edu/model-chemistry.

2.2. Deposition Velocities

Dry deposition velocities for ozone are loosely based on the work of *Galbally and Roy* [1980] and adjusted to produce a global average surface ozone mixing ratio of 30 ppbv. Dry deposition velocities for PAN, NO, and several other species are based on *Kotamarthi and Carmichael* [1990]. These dry deposition values are fixed for the simulation period because no representation of boundary layer processes is introduced into the model.

Wet deposition rates are scaled to the seasonal, climatological rainfall rates at the surface for each of the model latitude boxes. Washout rates for highly soluble species such as HNO_3 and H_2O_2 are set equal to the rainfall rates. Washout rates for other gases are set according to available data on Henry's law constant.

2.3. Emission Rates

The surface emissions of isoprene were obtained from the Global Emission Inventory Activity [*Guenther et al.*, 1995]. The emissions for C_2H_6 were based on *Rudolph* [1995], for acetone were based on *Singh et al.* [1995] and *McKeen et al.* [1997] and for propane, ethene, and propene were based on *Strand and Hov* [1994]. Table 1 gives the surface emissions for NO_x, CO, and all of the NMHCs used in the model. The latitudinal

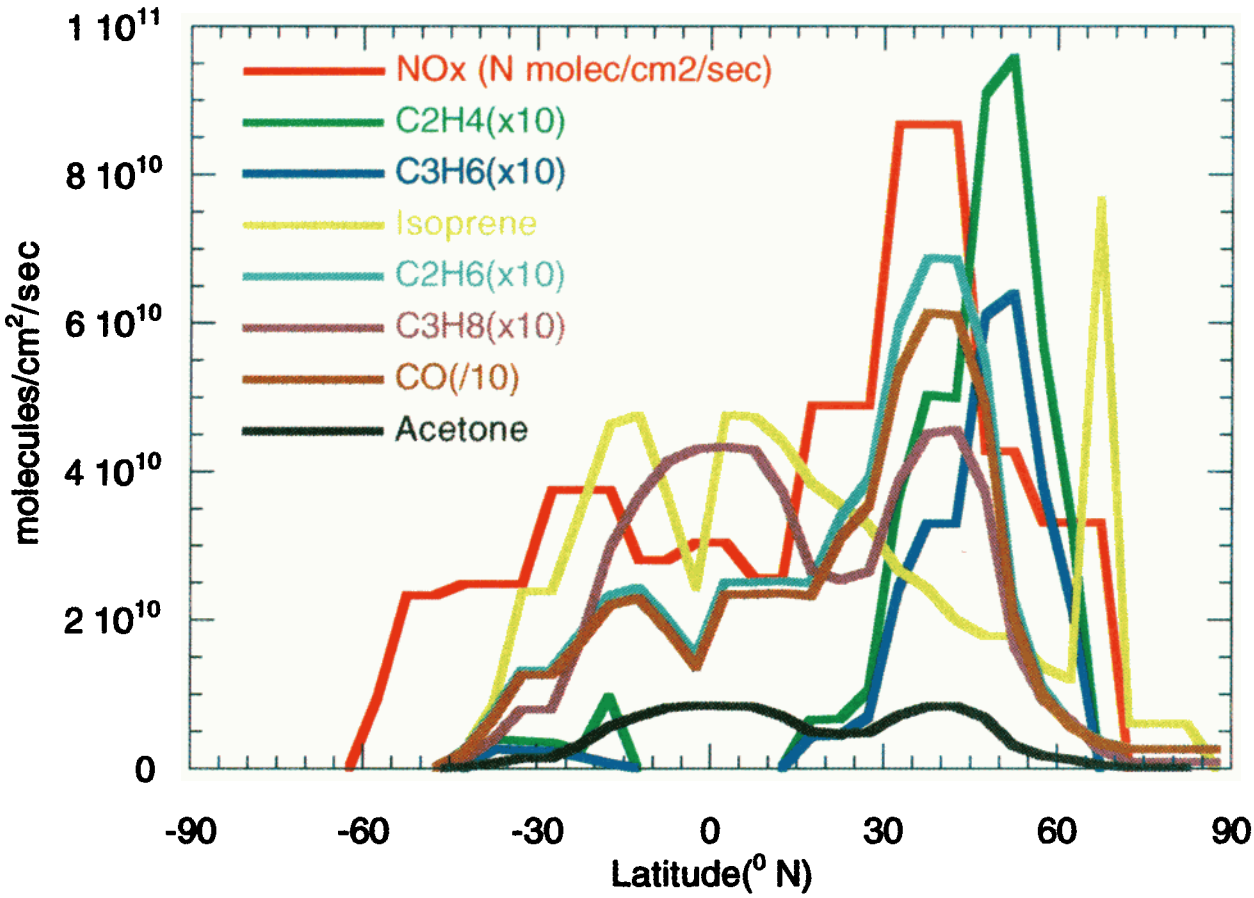

Plate 1. Latitudinal distribution of the surface flux emissions for the trace gases with specified flux boundary conditions in the model. The emissions of NO_x are reported as molecules of nitrogen. Scaling factors as indicated next to the plot labels are used to increase the readability of the plot.

distribution of surface flux emissions used in the model is shown in Plate 1. Additional NO_x emissions from lightning (5 Tg yr^{-1} of N) and from subsonic aircraft (0.5 Tg yr^{-1}) are included. The lightning source is distributed in the latitude and altitude domain as described by *Price et al.* [1997].

3. Results

In the next section we discuss the model's ability to reproduce observed distributions of C_2H_6, C_3H_8, and acetone. This is followed by an analysis of the impacts of (1) acetone on HO_x production rates and (2) NMHCs on ozone budgets in the troposphere. Finally, we examine an atmospheric chemical perturbation of current and future interest to the atmospheric chemistry community. Examined are the effects of a possible doubling of methane mixing ratios at the surface on tropospheric ozone mixing ratios.

The model characteristics in terms of key tropospheric components NO_x and NO_y are discussed in this section. Figure 1a shows the modeled NO_x for winter and summer months at three different altitude bins corresponding to lower troposphere (0–2 km), middle troposphere (2–7 km), and upper troposphere (7–12 km). There is a large variability in the measured NO_x in the troposphere with strong seasonal, diurnal, and regional influences. Since the zonal average model is representative of only the zonally averaged atmosphere, any attempt to verify the model with measured NO_x from any particular campaign would be ill advised. This aside, the calculated NO_x in the middle and upper troposphere are comparable to measurements made during the different campaigns. For completeness the vertical profile for NO_y at the equator is shown in Figure 1b. The data from the Stratospheric Tropospheric Exchange Project (STEP) campaign was com-

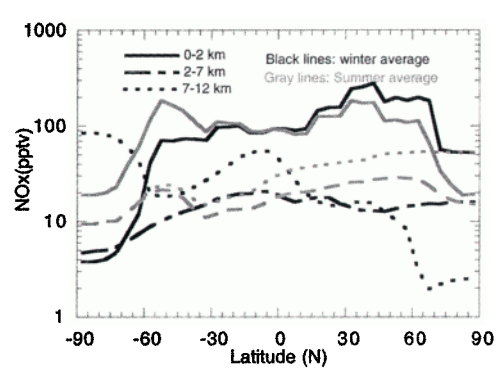

Figure 1a. Model-calculated NO_x in three altitude bins corresponding to the lower, middle, and upper troposphere. Results are shown as summer (June, July, and August) and winter (December, January, and February) averages.

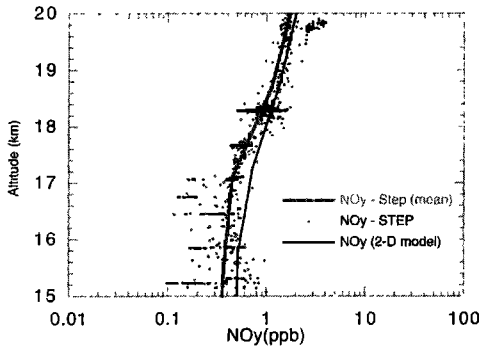

Figure 1b. Model-calculated and measured NO_y during the Stratospheric Tropospheric Exchange Project (STEP) in 1987. Model values represent the average for the tropical region defined as 30°N to 30°S latitude.

piled as discussed by *Kotamarthi et al.* [1994]. The mean values for the STEP data are obtained by binning the data into a series of 2-km altitude bins starting at a height of 5 km and extending to a height of 21 km. Figure 1c shows a comparison of the modeled and measured NO for the fall period corresponding to the Pacific Exploratory Mission (PEM)-WEST A period. The measurements include data reported from all flights and filtered to contain measurements made in "marine" air as described by *Talbot et al.* [1996]. The PEM-WEST data set represents a fair portion of the middle and lower latitude upper tropospheric data in the recently compiled climatology of nitrogen oxides reported by *Emmons et al.* [1997]. PEM-WEST A was chosen here for this comparison because of the larger number of data points that could be labeled as from relatively clean marine air origins during this period as compared to, for instance, the PEM-WEST B period [*Hoell et al.*, 1998]. Besides, it is hoped that the marine air is a better representation of a zonal mean average than fresh plumes coming from the continental areas. Considering the large variability of nitrogen oxides in the troposphere, the modeled mixing ratios can be considered to be a fair representation of

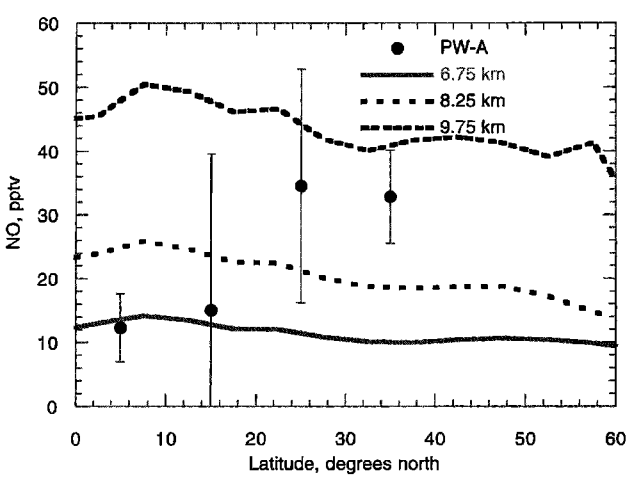

Figure 1c. Model-calculated and measured NO for the Pacific Exploratory Mission (PEM)-WEST A fall 1991 period. Measured data are filtered to represent air samples that have not been impacted by fresh emissions from the continental pollution and thus are considered to be marine air.

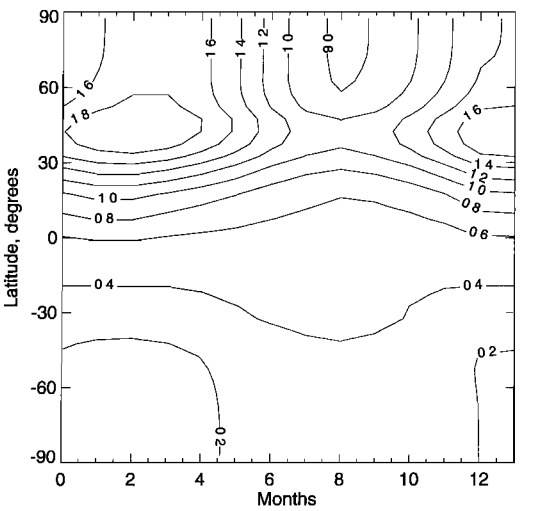

Figure 2. Calculated ethane mixing ratios at the surface (ppbv) as a function of latitude and season.

the zonal mean nitrogen oxide climatology in the upper troposphere.

3.1. Ethane

Model simulation of ethane and propane with 2-D tropospheric models was discussed by *Singh et al.* [1994]. *Rudolph* [1995] evaluated all available measurements of C_2H_6 to that time and estimated a global average surface mixing ratio of 800 pptv leading to an estimated global emission rate of 15 Tg yr^{-1} of ethane. *Rudolph* [1995] estimated emissions of ethane scaled to a C_2H_6 loss due to reaction with OH for a global average OH value of 6.4×10^5 molecules cm^{-3}. Because the currently estimated global average value of OH is 20% greater than this value and our model produces a CH_3CCl_3 lifetime approximately equal to the 4.9-year lifetime obtained by *Prinn et al.* [1995], we scaled these emissions up by 20%. The model simulation agrees with measurements in several respects, our calculated global and annual average C_2H_6 is 530 pptv, and the surface average mixing ratio is 802 pptv. The distribution of C_2H_6 at the model surface for the different months of the year is shown in Figure 2. The vertical distributions for September and February for 0–60°N are in good agreement with those reported by *Blake et al.* [1996, 1997]. Figure 3 shows the model-calculated and measured values of C_2H_6 for the month of March corresponding to the PEM-WEST B period [*Blake et al.*, 1997]. The model values are for the altitude bin centered at ~9 km, and the data represent the mean value and 1 standard deviation for the hydrocarbon data collected in the altitude bin at 7–11 km [*Blake et al.*, 1997]. The agreement is good from the equator to 60°N and within the error bars of the measurements. The measurements were filtered to remove the air presumed to be influenced by stratospheric air. The procedure used to identify the stratospheric air is the same as that described by *Kotamarthi et al.* [1997]. The seasonal cycle (change from maximum to minimum) in the C_2H_6 mixing ratio at the model surface is of the order of 1 ppb at ~50°N and 450 pptv at 15°N. These numbers are comparable to those reported by *Jobson et al.* [1993] for Faserdale, Canada (50°N), and by *Rudolph* [1995] for 14°N.

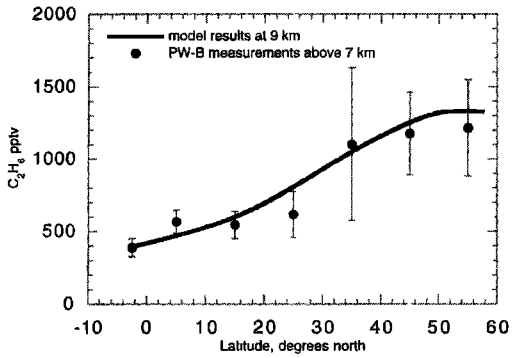

Figure 3. Calculated and measured ethane mixing ratios for the month of March (ppbv). Measurements are from the PEM-WEST B campaign as reported by *Blake et al.* [1997]. The measured values shown are the mean and 1 standard deviation for the altitude bin 7–12 km from all flights. Model results are from an altitude bin centered at ~9 km.

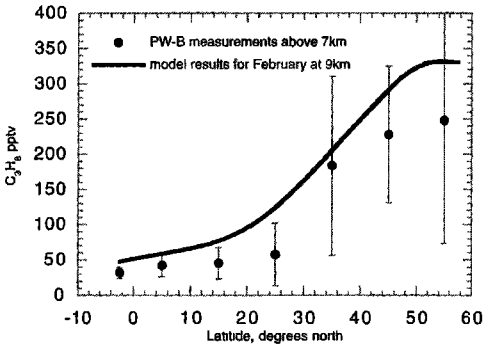

Figure 5. Calculated and measured propane mixing ratios for the month of March (pptv). Measurements are from the PEM-WEST B campaign as reported by *Blake et al.* [1997]. The measured values shown are the mean and 1 standard deviation for the altitude bin 7–12 km from all flights. Model results are from an altitude bin centered at ~9 km.

3.2. Propane

The global average propane mixing ratio calculated by the model is 107 pptv, and the surface average mixing ratio is calculated at 280 pptv. The distribution of C_3H_8 at the model surface for the different months of the year is shown in Figure 4. The surface level values are in general agreement with the data reported by *Kanakidou et al.* [1991]. The seasonal cycle for propane is 513 pptv in the midlatitude Northern Hemisphere (50°N) and ~90 pptv in the tropical region (15°N). The vertical distributions for September and February for 0–60°N are in good agreement with those reported by *Blake et al.* [1996, 1997]. Figure 5 shows the model-calculated and measured values of C_3H_8 for the month of March, corresponding to the PEM-WEST B period. The altitude and latitude bins for the model and measurements are as described for Figure 3. Again, the agreement between the model and measurements is good in the tropics to midlatitudes. The data were filtered to remove measurements influenced by air of recent stratospheric origin as discussed in the previous section.

3.3. Acetone

Acetone emissions of 40 Tg yr^{-1} of C were estimated by *McKeen et al.* [1997]. In the present simulation, surface acetone emissions are set at 65 Tg yr^{-1} of acetone. An additional 24 Tg yr^{-1} of acetone is produced from the oxidation of propane, thus contributing 27% of the total acetone emissions in the model. These values produced a global average mixing ratio of 572 pptv for acetone in the model, with 10% of the burden calculated to be due to the oxidation of propane. Annual average acetone profiles for the globe and the midlatitude Northern Hemisphere are presented in Figure 6. The latitudinal distribution of acetone emissions used in the model is shown in Plate 1.

Figure 7a shows the model-calculated acetone at ~9 km during the month of February in the Northern Hemisphere and the approximate mean measured values of acetone in the altitude range of 7–10 km during PEM-WEST B [*Singh et al.*, 1995]. The agreement between the modeled and measured values is good to 40°N and less so from 40° to 50°N. The PEM-WEST B data were filtered to remove air influenced by recent air of stratospheric origin as discussed in section 3.1.

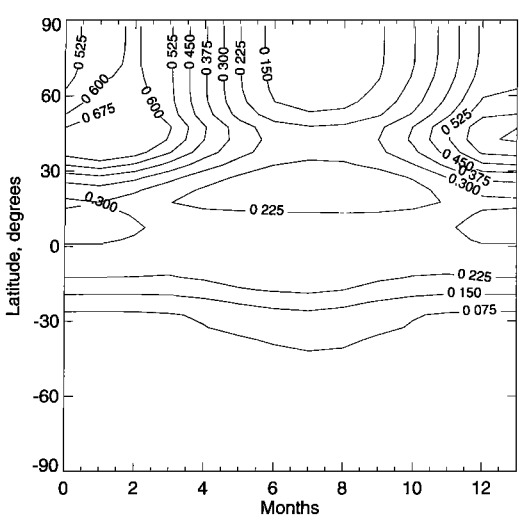

Figure 4. Calculated propane mixing ratios at the surface (parts per trillion (pptv)) as a function of latitude and season.

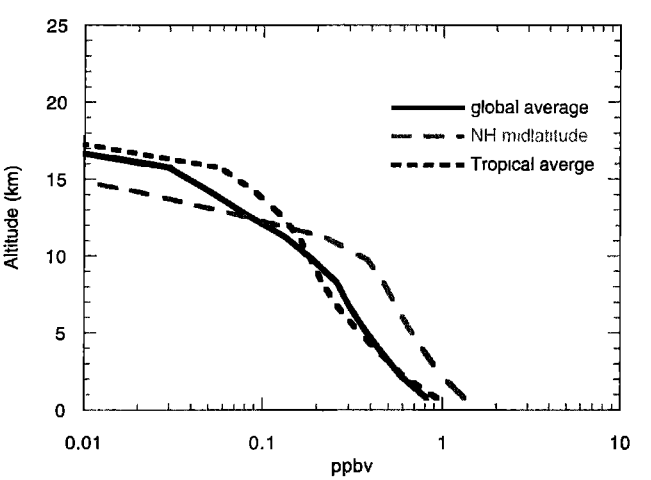

Figure 6. Annual calculated acetone mixing ratio profiles (pptv) as a global average, Northern Hemisphere midlatitude average (30°–60°N), and the tropical (30°N–30°S) average.

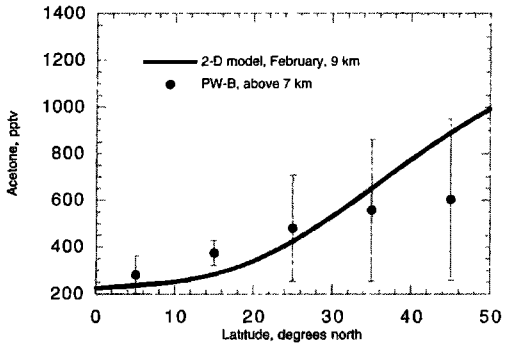

Figure 7a. Calculated acetone mixing ratios for February from the model for an altitude bin centered at ~9 km. Measured data are from PEM-WEST B campaign as reported by *Singh et al.* [1995]. Plotted are the mean and 1 standard deviation for a 10° latitude band and the altitude bin corresponding to 7–10 km from all flights.

Figure 7b shows the measured values of acetone from the Pollution in the North Atlantic Flight Corridor (POLINAT) program, as reported by *Arnold et al.* [1997] for the latitude range of 66°–73°N and for the month of February. Although the model values are closer to measurements in the troposphere, the measured values in the lower stratosphere are much higher than those calculated with the model. Figure 7c shows the measured and calculated values of acetone in the lower and middle troposphere at 45°–65°N in August during Arctic Boundary Layer Expedition (ABLE) 3B [*Singh et al.*, 1994]. The measured values are higher by 20–50% than calculated values. However, many of these measured values are influenced by local pollution events because the data were collected during continental outflow conditions, close to the continental shelf, and show large variations. Measured values in clean air at an altitude of 5 km [*Singh et al.*, 1994] are much closer to the calculated values.

In general, the calculated acetone values are in reasonable agreement with measured values for clean air measurements but are much lower near the continental troposphere. This is expected because the 2-D zonal average model cannot reproduce the zonal structure observed in the measurements.

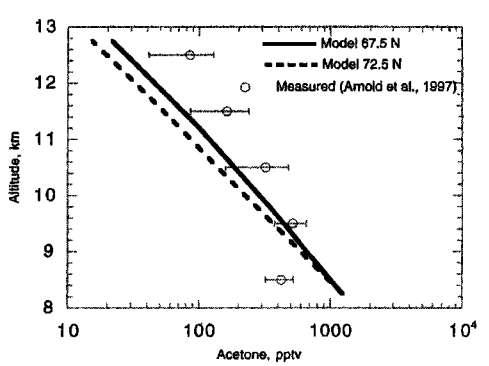

Figure 7b. Calculated acetone mixing ratios for February from the model for latitude bins centered at 72.5° and 67.5°N. Measured data are from the Pollution in the North Atlantic Flight Corridor (POLINAT) campaign as reported by *Arnold et al.* [1997]. Plotted are the mean and 1 standard deviation for a 10° latitude band extending from 65° to 75°N.

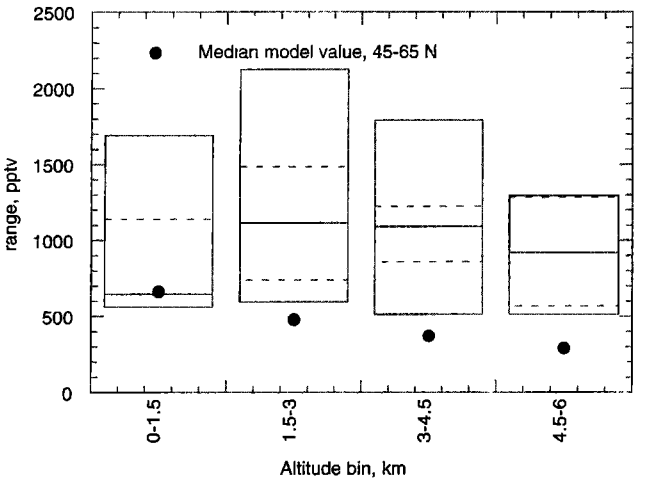

Figure 7c. Calculated acetone mixing ratios for August from the model for latitude bin extending from 45° to 65°N. Measured data are from the Arctic Boundary Layer Expedition (ABLE) 3B campaign as reported by *Singh et al.* [1994]. Plotted are the mean and 1 standard deviation from all flights.

3.3.1. Seasonal average and annual average impacts of acetone on HO_x. Acetone has been proposed as a major source of HO_x in the upper troposphere by *Singh et al.* [1995], *Jaegle et al.* [1997], *McKeen et al.* [1997], and *Arnold et al.* [1997]. Here we present a global-scale evaluation of the impacts of the photolysis of acetone on HO_x production rates in the troposphere and lower stratosphere. The photolysis of acetone produces CH_2O and HO_2. Each molecule of acetone photolyzed is expected to produce 2.3 molecules of HO_x [*Singh et al.*, 1995]. *Singh et al.* [1995] and *Arnold et al.* [1997] gave detailed accounts of the chemical pathways producing HO_x from acetone and the fractional yields. Below we discuss the production rates of HO_x from acetone calculated by using the zonally averaged model on spatial scales ranging from regional to global and timescales extending from seasonal to annual. All of the HO_x production rates discussed below are calculated on the basis of diurnally averaged photolytic rates, thermal reaction rates, and mixing ratios.

3.3.2. Seasonal and regional impacts. Figure 8 shows the annual averaged contributions of key processes to HO_x production rates for the midlatitude Northern Hemisphere (30°–60° N) and tropical regions (30°S to 30°N). The greatest impact

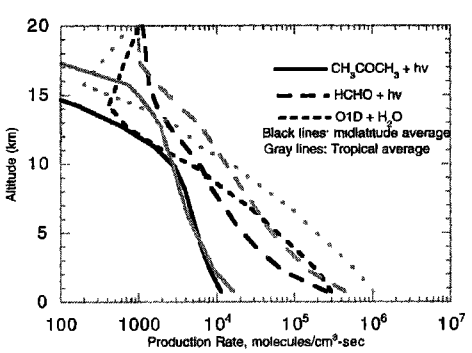

Figure 8. HO_x production rates from three key process as calculated by the model. Calculations were averaged for one full year in a latitude band extending from 30° to 60°N (solid lines) and from 30°S to 30°N (shaded lines).

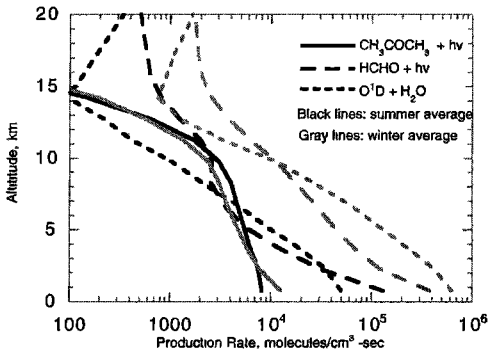

Figure 9. HO_x production rates for three key process, as calculated by the model. Calculations were averaged for the summer months (June, July, and August) in a latitude band extending from 30° to 60°N (solid lines) and for winter months (December, January, and February) (shaded lines).

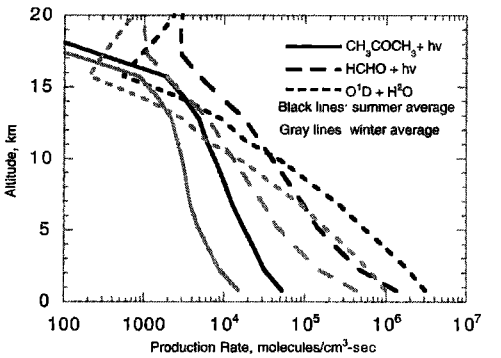

Figure 10. HO_x production rates from three key process as calculated by the model. Calculations were averaged for the summer months (June, July, and August) in a altitude band extending from 30° to 30°N (solid lines) and for winter months (December, January, and February) (shaded lines).

on HO_x production rates due to the introduction of acetone into the model occurs in the upper troposphere and lower stratosphere, with maximum changes occurring in the tropical upper troposphere. For these two regions, however, CH_2O produced by the oxidation of CH_4 is the major contributor followed closely by acetone for the tropical regions and contributions of $O(^1D) + H_2O$ and acetone for the Northern Hemisphere midlatitude regions.

The effects for the winter (average for the months of December, January, and February) are more dramatic in the midlatitude, as expected (Figure 9). During this period, acetone mixing ratios in excess of 500 pptv are available in the middle and upper troposphere (Figures 6 and 7); these ratios, combined with reduced efficiency of the $O(^1D) + H_2O$ cycle due to the decreased UV fluxes, lead to dramatic shifts in the contributions of these three processes to the HO_x production rates. For much of the middle and upper troposphere, acetone becomes the largest contributor to HO_x production rates.

For summer months (June, July, and August) the net contribution of the acetone pathway to HO_x production rates decreases in the midlatitude Northern Hemisphere, becoming smaller than both $O(^1D) + H_2O$ and CH_4-derived CH_2O. This change results from lower acetone concentrations in the upper troposphere, reflecting increased losses in the lower troposphere by reaction with OH in the summer months (Figure 9). In addition, the contribution from $O(^1D) + H_2O$ increases because of the increased UV flux available, providing an additional mechanism for reducing the impact of the acetone pathway.

The tropical belt shows no significant deviation from the annual behavior (Figure 10), indicating little seasonality in the calculated HO_x production rates for this region. The global average HO_x production pathways for summer and winter months show no significant seasonal cycle. The contribution from the acetone cycle in the upper and midlatitude troposphere is slightly higher in the summer months than in the winter months and is similar to that in tropical regions.

3.4. Ozone Changes

Introducing hydrocarbons into the 2-D zonal average model increases the ozone concentrations in the modeled troposphere and lower stratosphere. As discussed in section 1.2, hydrocarbons increase the ozone production potential in the atmosphere. In this calculation the highest increases occur in the tropical upper troposphere and lower stratosphere. Figures 11 and 12 show the calculated increases in ozone with altitude for January and July, respectively. Both show similar increases in ozone with altitude and latitude. The tropical upper troposphere now has additional HO_x available in the model from acetone photolysis. This increases the ozone from an enhancement in the conversion rate of the $NO + HO_2$ reaction rate, resulting in the conversion of NO to NO_2. However, there is also an increase in the loss of ozone by the $O_3 + HO_2$ reaction pathway. At 10-km altitude, on a global and annual average basis, the main loss mechanism for ozone in the model is the reaction of ozone with HO. This pathway is greater by a factor of 2 than the reaction of ozone with HO_2. Higher HO_2 at this altitude in the model, which is due to acetone photolysis, increases the ozone + HO_2 reaction rate by 27%, an insignificant amount compared to the dominant ozone + OH reaction. Thus there is no significant change in the loss rate of ozone. The ozone production rate at this same altitude is dominated by the $NO + HO_2$ reaction pathway, converting NO to NO_2 and forming nearly 83% of the model production rate term for ozone at this altitude. The extra HO_2 from acetone photolysis also increases the production rate due to this term by 27%. Thus the net effect, an increase of nearly 27% in the net ozone chemical production tendency in this altitude region, results in

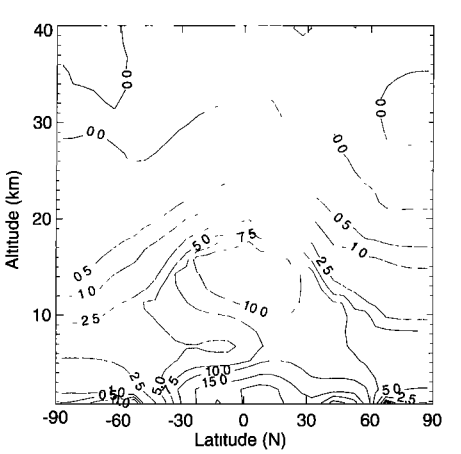

Figure 11. Percent change in ozone mixing ratios for January as a result of including nonmethane hydrocarbon chemistry in the model.

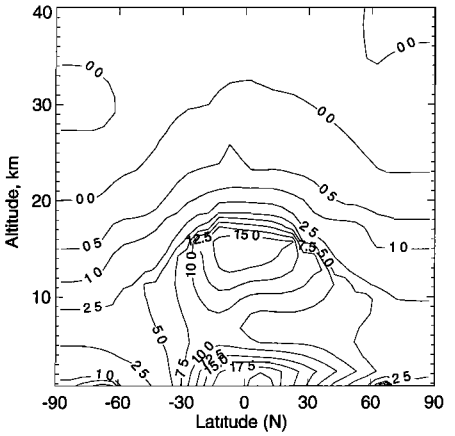

Figure 12. Percent change in ozone mixing ratios for July as a result of including nonmethane hydrocarbon chemistry in the model.

a net increase of ozone in the upper troposphere and lower stratosphere.

Ozone increases by rates ranging from 4 to 0.5% in Northern Hemisphere midlatitudes and at altitudes above 10 km (which represents the lower stratosphere in our model) because of the inclusion of hydrocarbons. Increases ranging from 2% in the tropics to 0.5% in the high latitudes are obtained at 18.5 km, which is the first grid box entirely in the stratosphere for the entire model domain for all seasons. The changes in ozone in the Northern Hemisphere midlatitudes are largely due to the introduction of C_2H_6 and the subsequent formation of PAN, whereas the major contributor to the increase of ozone in the tropical region is the introduction of acetone into the model (Figure 12).

On a global and annual average, ozone in the model increases by 5 ppbv in the lower troposphere and by close to 10 ppbv in the upper troposphere and lower stratosphere because of the introduction of hydrocarbons into the model (Figure 13). The net tendency for ozone chemical production is slightly more negative in the middle troposphere and fractionally more positive in the lower troposphere, upper troposphere, and lower stratosphere because of the introduction of hydrocarbons. Thus the calculated increases in ozone mixing ratio in the middle troposphere result largely from transport from the upper troposphere.

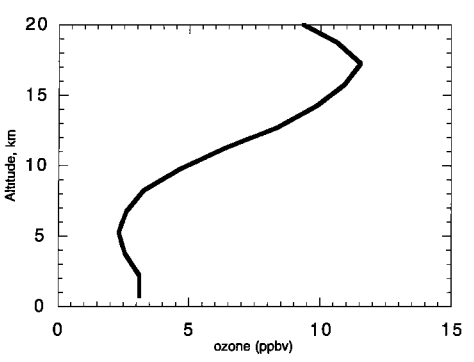

Figure 13. Additional ozone produced (ppbv) on a global and annual average basis in the troposphere as a result of introducing nonmethane hydrocarbon chemistry into the model.

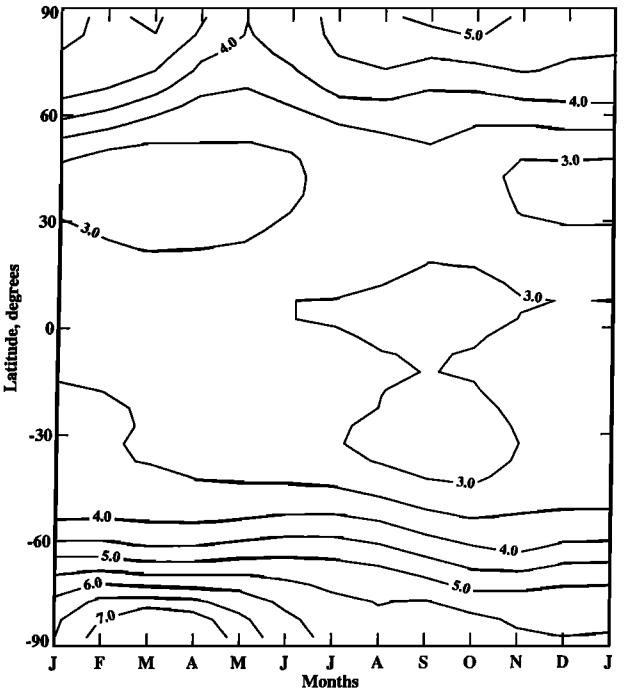

Figure 14. Percent change in column ozone calculated with the model by a doubling of the surface mixing ratio of CH_4.

3.5. Methane Doubling Scenario Calculations and the Effect of Including NMHCs in the Model

In the next 100 years, depending on changes in emissions, the surface level mixing ratios of methane could double from the current 1.7 to 3.4 ppm [*WMO*, 1995]. Methane is an important greenhouse gas, besides playing a key role in the chemistry of the troposphere. Several assessment studies conducted with the IPCC and WMO evaluation's over the past decade used state-of-the-art chemical transport models to evaluate the effects of CH_4 increases on tropospheric oxidizing capacity and expected CH_4 mixing ratios in the entire atmosphere. The most recent such evaluation was for the *WMO* [1995]. Here we present model results for a CH_4 doubling scenario and the effects of including the current set of NMHCs on the expected perturbation in ozone mixing ratios under this scenario.

Figure 14 gives the changes in total ozone as a function of latitude and season, calculated with the current version of the 2-D zonal average model, with NMHCs included. This calculation resulted in a 3.4% increase in globally averaged total ozone with a doubling of CH_4.

The calculations for increased CH_4 give a small percentage increase in lower stratospheric ozone, a larger increase near 40-km altitude, and a decrease above 45 km. The hydrogen oxides produced by CH_4 oxidation affect the efficiency of the NO_x and ClO_x catalytic ozone destruction mechanisms [*Wuebbles et al.*, 1999] in the stratosphere. In the upper stratosphere the additional HO_x reacts catalytically with ozone, leading to the decrease in ozone determined at these altitudes in the model calculations.

The impact of including hydrocarbons in a doubled CH_4 scenario is shown in Figure 15. The change in column ozone resulting from a doubled CH_4 without hydrocarbons in the model is an increased response by 3–8% over the case with NMHCs in the calculations. The effect in the Southern Hemi-

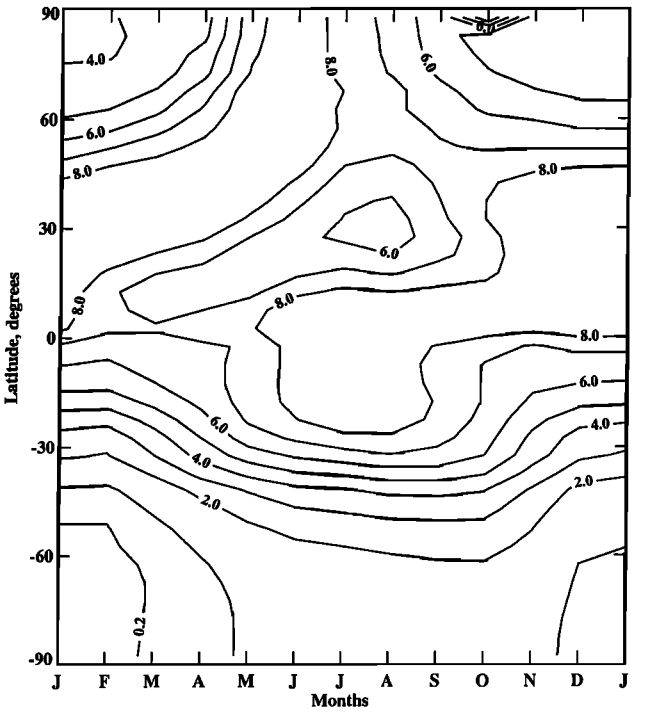

Figure 15. Reduction (percent) in the change in the model column ozone due to doubled CH_4 as a result of introducing nonmethane hydrocarbon chemistry into the model.

sphere is negligible because there are no significant NMHC emissions from this region. Thus the model response to a double CH_4 scenario in the Northern Hemisphere is damped when NMHCs are included in the model. This reflects the additional hydrocarbon sources of RO_2 in the lower troposphere and decreases the impact of doubling CH_4 in this region. The current model gives a feedback factor, defined as the percent change in OH for a 1% change in CH_4 [*WMO*, 1995], of 0.32%, which is within the range calculated by *WMO* [1995].

4. Conclusions

We explored the effects of including a limited set of NMHCs in a well-established 2-D zonal average model that is frequently used for assessment studies on topics such as the impacts of high speed civil transports (HSCTs), replacement chlorofluorocarbons, ozone depletion potentials, lifetimes of CFCs and HCFCs, and several other applications. The NMHC chemistry was selected to represent the most important possible contributors to a 2-D zonal average model in terms of their lifetimes and those of their degradation products. The species chosen have lifetimes ranging from less than a day to a few months.

Acetone was shown to have a significant impact on HO_x production rates throughout the year in the upper tropical troposphere. The midlatitude Northern Hemisphere is affected the most during the winter months. The additional HO_x in the modeled upper troposphere leads to additional ozone production, ranging up to 10%. The impacts of these hydrocarbons were, however, found to be much smaller in the lower stratosphere, with changes in production of an additional 2% ozone or less.

The introduction of these NMHCs in the model was also shown to affect commonly used assessment scenarios such as CH_4 doubling. The NMHCs damp the response of the model in terms of ozone change. The CH_4 doubling scenario with NMHCs produced 2–8% less change in column ozone than the no-NMHC case. Because the 2-D zonal average models find selected applications in the assessment of tropospheric processes, a minimum set of NMHCs should be included. Using the results from the 3-D CTMs to select the hydrocarbon species of possible relevance to 2-D zonal average models might be useful.

Acknowledgments. This work was partially supported by the U.S. Department of Energy, the Office of Energy Research, the Office of Biological and Environmental Research, the Environmental Sciences Division, as a part of the Atmospheric Chemistry Program, and NASA under the ACMAP. We also thank the reviewers for their suggestions and help in improving the presentation.

References

Arnold, F., V. Burger, B. Droste-Franke, F. Grimm, A. Krieger, J. Schneider, and T. Stilp, Acetone in the upper troposphere and lower stratosphere: Impact on trace gases and aerosols, *Geophys. Res. Lett.*, *24*, 3017–3020, 1997.

Atkinson, R., D. L. Baulch, R. A. Cox, R. F. Hampson, J. A. Kerr, M. J. Rossi, and J. Troe, Evaluated kinetic photochemical and heterogeneous data for atmospheric chemistry: Supplement V, IUPAC Subcommittee on Gas Kinetic Data evaluation for atmospheric chemistry, *J. Phys. Chem. Ref. Data*, *26*, 521–1012, 1997.

Atlas, E., S. M. Schauffler, J. T. Merrill, C. J. Hahn, B. Ridley, J. Walega, J. Greenberg, L. Heidt, and P. Zimmerman, Alkyl nitrate and selected halocarbon measurements at Mauna Loa observatory, Hawaii, *J. Geophys. Res.*, *97*, 10,331–10,348, 1992.

Baughcum, S. L., Subsonic aircraft emission inventories, in *Atmospheric Effects of Aviation: First Report of the Subsonic Assessment Project, NASA Ref. Publ. 1385*, 15–29, 1996.

Blake, D. R., T.-Y. Chen, T. W. Smith, C. J.-L. Wang, O. W. Wingenter, N. J. Blake, F. S. Rowland, and E. W. Mayer, Three-dimensional distribution of nonmethane hydrocarbons and halocarbons over the northwestern Pacific during the 1991 Pacific Exploratory Mission (PEM-West A), *J. Geophys. Res.*, *101*, 1763–1778, 1996.

Blake, D. R., T.-Y. Chen, T. W. Smith, C. J.-L. Wang, O. W. Wingenter, N. J. Blake, F. S. Rowland, and E. W. Mayer, Three-dimensional distribution of nonmethane hydrocarbons and halocarbons over the northwestern Pacific during the 1991 Pacific Exploratory Mission (PEM-West B), *J. Geophys. Res.*, *102*, 11,763–11,778, 1997.

Brasseur, G. P., D. A. Hauglustaine, S. Walters, P. J. Rasch, J.-F. Muller, C. Granier, and X. X. Tie, MOZART; A global chemical transport model for ozone and related chemical tracers, 1, Model description, *J. Geophys. Res.*, *103*, 28,265–28,289, 1998.

Chang, J. S., A. Brost, I. S. A. Isaksen, S. Madronich, P. Middleton, W. R. Stockwell, and C. J. Walcek, A three-dimensional Eulerian acid deposition model: Physical concepts and formulation, *J. Geophys. Res.*, *92*, 14,681–14,700, 1987.

DeMore, W. B., S. P. Sander, D. M. Golden, R. F. Hampson, M. J. Kurylo, C. J. Howard, A. R. Ravishankara, C. E. Kolb, and M. J. Molina, Chemical kinetics and photochemical data for use in stratospheric modeling: Evaluation number 12, *Jet Propul. Lab. Publ 97-4*, Natl. Aeronaut. and Space Admin., Pasadena, Calif., 1997.

Emrich, M., and P. Warneck, Photodecomposition of Acetone, in *Mechanisms of Gas Phase and Liquid Phase Chemical Transformations in Tropospheric Chemistry*, edited by R. A. Cox, *EUR 12035*, pp. 29–32, Eur. Union, Brussels, 1988.

Emmons, L. K., et al., Climatologies of NO_x and NO_y: A comparison of data and models, *Atmos. Environ.*, *31*, 1851–1904, 1997.

Fukui, Y., and P. V. Doskey, Air-surface exchange of nonmethane organic compounds at a grassland site: Seasonal variations and stressed emissions, *J. Geophys. Res.*, *103*, 13,153–13,168, 1998.

Galbally, I. E., and C. R. Roy, Destruction of ozone at the Earth's surface, *Q. J. R. Meteorol. Soc.*, *106*, 599–620, 1980.

Guenther, A., et al., A global model of natural volatile organic compound emissions, *J. Geophys. Res.*, *100*, 8873–8892, 1995.

Hoell, J. M., D. D. Davis, S. C. Liu, R. E. Newell, H. Akimoto, R. J. McNeal, and R. J. Bendura, The Pacific Exploratory Mission-West Phase B, *J Geophys. Res.*, *102*, 28,223–28,239, 1997.

Hough, A. M., The development of a two-dimensional tropospheric model, the model chemistry, *J. Geophys. Res.*, *96*, 7325–7362, 1991.

Houweling, S., F. Dentener, and J. Lelieveld, The impact of nonmethane hydrocarbon compounds on tropospheric photochemistry, *J. Geophys. Res.*, *103*, 10,673–10,696, 1998.

Jacob, D. J., et al., Evaluation and intercomparison of global atmospheric transport models using ^{222}Rn and other short-lived tracers, *J. Geophys. Res.*, *102*, 5953–5970, 1997.

Jaegle, L., et al., Observed OH and HO_2 in the upper troposphere suggest a major source from convective injection of peroxides, *Geophys. Res. Lett.*, *24*, 3181–3184, 1997.

Jobson, B. T., Z. Wu, H. Niki, and L. A. Barrie, Seasonal trends of isoprene, C_2–C_5 alkanes and acetylene at a remote boreal site in Canada, *J. Geophys. Res.*, *98*, 16,893–16,901, 1993.

Kanakidou, M., H. B. Singh, K. M. Valentin, and P. J. Crutzen, A two-dimensional model study of ethane and propane oxidation in the troposphere, *J. Geophys. Res.*, *96*, 15,395–15,413, 1991.

Kasting, J. F., and H. B. Singh, Non-methane hydrocarbons in the troposphere: Impact on odd hydrogen and odd nitrogen chemistry, *J. Geophys. Res.*, *91*, 13,239–13,256, 1986.

Kinnison, D. E., D. J. Wuebbles, and H. S. Johnston, Model study of atmospheric transport using carbon-14 and strontium-90 as inert tracers, *J. Geophys. Res.*, *99*, 20,647–20,664, 1994.

Kotamarthi, V. R., and G. R. Carmichael, The long range transport of pollutants in the Pacific rim region, *Atmos. Env.*, *24A*, 1521–1534, 1990.

Kotamarthi, V. R., M. K. W. Ko, D. K. Weisenstein, J. M. Rodriguez, and N. D. Sze, The effect of lightning on the concentration of odd nitrogen species in the lower stratosphere: An update, *J. Geophys. Res.*, *99*, 8167–8173, 1994.

Kotamarthi, V. R., J. M. Rodriguez, N. D. Sze, Y. Kondo, R. Pueschel, G. Ferry, S. Sandholm, G. Gregory, D. Davis, and S. Liu, Evidence of heterogeneous chemistry on sulfate aerosols in stratospheric air masses measured in PEM-West B, *J. Geophys. Res.*, *102*, 28,425–28,436, 1997.

Langner, L., H. Rodhe, and M. Olofsson, Parameterization of subgrid scale vertical transport in a global two-dimensional model of the troposphere, *J. Geophys. Res.*, *95*, 13,691–13,706, 1990.

Li, L., T. R. Nathan, and D. J. Wuebbles, Topographically forced planetary wave breaking in the stratosphere, *Geophys. Res. Lett.*, *22*, 2953–2956, 1995.

Liu, S. C., M. Trainer, F. C. Fehsenfeld, D. D. Parrish, E. J. Williams, D. W. Fahey, G. Hubler, and P. C. Murphy, Ozone production in the rural troposphere and the implications for regional and global ozone production, *J. Geophys. Res.*, *92*, 4191–4207, 1987.

McKeen, S. A., E.-Y. Hsie, M. Trainer, R. Tallamraju, and S. C. Liu, A regional model study of the ozone budget in the eastern United States, *J. Geophys. Res.*, *96*, 10,809–10,845, 1991.

McKeen, S. A., P. Wennberg, T. Gierczak, J. B. Burkholder, E. Keim, A. R. Ravishankara, R. Gao, S. C. Liu, and D. Fahey, The photochemistry of acetone in the upper troposphere: A source of odd-hydrogen radicals, *Geophys. Res. Lett.*, *24*, 3177–3180, 1997.

Moxim, W. J., Simulated global tropospheric PAN: Its transport and impact on NO_x, *J. Geophys. Res.*, *101*, 12,621–12,638, 1996.

Muller, J.-F., and G. Brasseur, IMAGES: A three-dimensional chemical transport model for the global atmosphere, *J. Geophys. Res.*, *100*, 16,445–16,490, 1995.

Muthuramu, K., P. B. Shepson, J. W. Bottenheim, B. T. Jobson, H. Niki, and K. G. Anlauf, Relationships between organic nitrates and surface ozone destruction during polar sunrise experiment 1992, *J. Geophys. Res.*, *99*, 25,369–25,378, 1994.

Penkett, S. A., N. J. Blake, P. Lightman, A. R. W. Marsh, P. Anwyl, and G. Butcher, The seasonal variation of nonmethane hydrocarbons in the free troposphere over the North Atlantic Ocean: Possible evidence for extensive reaction of hydrocarbons with the nitrate radical, *J. Geophys. Res.*, *98*, 2865–2885, 1993.

Prather, M. J., and D. J. Jacob, A persistent imbalance in HO_x and NO_x photochemistry of the upper troposphere driven by deep tropical convection, *Geophys. Res. Lett.*, *24*, 3189–3192, 1997.

Prather, M. J., M. McElroy, S. Wofsy, G. Russell, and D. Rind, Chemistry of global troposphere: Fluorocarbons as tracers of air motion, *J. Geophys. Res.*, *92*, 6579–6613, 1987.

Price, C., J. Penner, and M. J. Prather, NO_x from lightning, 1, Global distribution based on lightning physics, *J. Geophys. Res.*, *102*, 5929–5941, 1997.

Prinn, R. G., R. F. Weiss, B. R. Miller, J. Huang, F. N. Alyea, D. M. Cunnold, P. J. Fraser, D. E. Hartley, and P. G. Simmonds, Atmospheric trends and lifetime of CH_3CCl_3 and global OH concentrations, *Science*, *269*, 187–192, 1995.

Ridley, B. A., E. L. Atlas, J. G. Walega, G. L. Kok, T. A. Staffelbach, J. P. Greenberg, F. E. Grahek, P. G. Hess, and D. D. Montzka, Aircraft measurements made during the spring maximum of ozone at Hawaii: Peroxides, CO, O3, NO_y, condensation nuclei, selected hydrocarbons, halocarbons, and alkyl nitrates between 0.5 and 9 km altitude, *J. Geophys. Res.*, *102*, 18,935–18,961, 1997.

Roberts, J. M., The atmospheric chemistry of organic nitrates, *Atmos. Environ., Part A*, *24*, 243–287, 1990.

Rudolph, J., The tropospheric distribution and budget of ethane, *J. Geophys. Res.*, *100*, 11,369–11,381, 1995.

Seinfeld, J. H., *Atmospheric Chemistry and Physics of Air Pollution*, John Wiley, New York, 1986.

Singh, H. B., and P. L. Hanst, Peroxyacetyl nitrate (PAN) in the remote unpolluted atmosphere: An important reservoir of nitrogen oxides, *Geophys. Res. Lett.*, *8*, 941–944, 1981.

Singh, H. B., D. O'Hara, D. Herlth, W. Sachse, D. R. Blake, J. D. Bradshaw, M. Kanakidou, and P. J. Crutzen, Acetone in the atmosphere: Distribution, sources and sinks, *J. Geophys. Res.*, *99*, 1805–1819, 1994.

Singh, H. B., M. Kanakidou, P. J. Crutzen, and D. J. Jacob, High concentrations and photochemical fate of oxygenated hydrocarbons in the global troposphere, *Nature*, *378*, 50–54, 1995.

Strand, A., and O. Hov, A two-dimensional zonally averaged transport model including convective motions and a new strategy for the numerical solution, *J. Geophys. Res.*, *98*, 9023–9037, 1993.

Strand, A., and O. Hov, A two-dimensional global study of tropospheric ozone production, *J. Geophys. Res.*, *99*, 22,877–22,895, 1994.

Wang, Y., D. J. Jacob, and J. A. Logan, Global simulation of tropospheric O_3-NO_x-hydrocarbon chemistry, 3, Origin of tropospheric ozone and effects of nonmethane hydrocarbons, *J. Geophys. Res.*, *103*, 10,757–10,767, 1998.

World Meteorological Organization (WMO), *Scientific Assessment of Ozone Depletion: 1991, Global Ozone Res. Monit. Proj. Rep. 25*, Geneva, 1992.

World Meteorological Organization (WMO), *Scientific Assessment of Ozone Depletion: 1994, Global Ozone Res. Monit. Proj. Rep. 37*, Geneva, 1995.

Wuebbles, D. J., D. E. Kinnison, K. E. Grant, and J. Lean, The effect of solar flux variations and trace gas emissions on recent trends in stratospheric ozone and temperature, *J. Geomagn. Geoelectr.*, *43*, 709–718, 1991.

Wuebbles, D. J., K. A. S. Hayhoe, and R. Kotamarthi, Methane in the global environment, in *Atmospheric Methane and Its Role in the Environment, NATO ASI Ser.*, edited by M. A. K. Khalil, Springer-Verlag, New York, in press, 1999.

V. R. Kotamarthi, Environmental Research Division, Argonne National Laboratory, Argonne, IL 60439. (vrkotamarthi@anl.gov)

R. A. Reck, National Institute for Global Environmental Change, University of California, Davis, CA 95616.

D. J. Wuebbles, Department of Atmospheric Sciences, University of Illinois at Urbana-Champaign, Urbana, IL 61801.

(Received October 21, 1998; revised May 12, 1999, accepted May 14, 1999.)